Available online at www.sciencedirect.com
SCIENCE DIRECT®
Nuclear Engineering and Design 225 (2003) 191–217
Nuclear Engineering and Design
www.elsevier.com/locate/nucengdes

Notes on the implementation of a fully-implicit numerical scheme for a two-phase three-field flow model

Cesare Frepoli [a,*], John H. Mahaffy [b], Katsuhiro Ohkawa [a]

[a] *Westinghouse Electric Co., P.O. Box 355, Monroeville, PA, USA*
[b] *The Pennsylvania State University, 237 Reber Bldg., University Park, PA, USA*

Received 23 October 2002; received in revised form 15 May 2003; accepted 12 June 2003

Abstract

The development of a fully-implicit scheme to model the two-phase three-field flow and heat transfer problem is presented here. The model was originally developed to simulate the complex phenomena occurring in proximity of the quench front of a nuclear reactor core during the reflood phase of a postulated LOCA. The fully-implicit method allows relative large time steps to be used even on very fine spatial grids which can not be considered when a semi-implicit scheme is applied to solve the conservation equation. The objective of this paper is to capture as much as possible, the lessons learned during the development and coding of the fully-implicit two-phase three-field model. The implementation of the model is one of the most time consuming and a challenging task. The literature on numerical models generally concentrates on the theoretical aspects of the numerical method but available information on the problems encountered during the implementation of such methods for real applications is scarce. The reason is that many of these methods are tailored to specific applications and sometimes are rather empirical. These techniques are the result of a long and tedious trial and error process from the developer. The article presented here attempts to provide some insights and guidelines for future development of this or similar models.

1. Introduction

During the last century significant progress has been made in modeling the complexity of the vapor/liquid two-phase flow. Two-phase computer codes are now widely used in many engineering fields. Several methods have been proposed and studied which can be found in the open literature. Large thermal-hydraulic system codes such as TRAC (Schnurr et al., 1990), RELAP (RELAP5 Code Development Team, 1995a,b) and COBRA series (Paik et al., 1985; Thurgood and George, 1983) are based on the semi-implicit scheme. The semi-implicit scheme has a rather simple implementation and has proved to be reasonably stable and accurate for most applications (Liles and Reed, 1978). The momentum equations couple the mass and energy equations only through new time pressure terms, and the difference equations can be reduced to a set of pressure equations (Thurgood and George, 1983, Vol. 3).

The shortcomings are that the stability is limited by the material Courant time step limit and the maximum allowable time step can become too small and impractical when a high spatial resolution is desired. TRAC and RELAP deal with the material Courant limit by adding the SETS (or Nearly Implicit) method (Mahaffy, 1982). However, other instabilities

* Corresponding author. Tel.: +1-412-374-4156; fax: +1-412-374-5139.
E-mail address: Frepolc@westinghouse.com (C. Frepoli).

0029-5493/$ – see front matter © 2003 Elsevier B.V. All rights reserved.
doi:10.1016/S0029-5493(03)00159-6

Nomenclature

Acronyms

ADI	alternate direction implicit
LOCA	loss of coolant accident
PWR	pressurized water reactor
CHF	critical heat flux
FVM	finite volume method
PDE	partial derivative equation
FLECHT	full length emergency core heat transfer
SEASET	system effect and separate effect tests

Symbols

$A'''_{i,d}$	droplets interfacial area concentration
D	diameter
g	gravity constant
h	enthalpy
P	pressure
q_{il}	interfacial heat transfer to the liquid
q_{iv}	interfacial heat transfer to the vapor
Q_{wl}	heat transfer from the wall to the liquid
Q_{wv}	heat transfer from the wall to the vapor
t	time
T	temperature
u	velocity
x	axial coordinate
S'''_E	volumetric source of entrainment
S'''_D	volumetric source of de-entrainment

Greek symbols

α	void fraction
η	droplet evaporation efficiency
ρ	density
σ	surface tension
τ	shear stress
Γ'''	volumetric vapor generation rate

Subscripts

a	donor value at the upper cell boundary (above)
b	donor value at the bottom cell boundary (below)
C	condensation
d	droplet
D	de-entrainment
e	entrainment
E	evaporation
f	liquid at saturation
g	vapor at saturation
i	interfacial
j	index cell
l	liquid
v	vapor
ve	vapor to entrainment
vl	vapor to liquid
w	wall
wv	wall to vapor
wl	wall to liquid

Superscripts

n	old time level
$n+1$	new time level

associated with the closure relationships of the two-phase flow require the implementation of time-smoothing techniques in order to stabilize the solution. Because friction and heat transfer coefficients (wall and interfacial) are evaluated explicitly, even with the time-smoothing, bounded instabilities produce unphysical oscillations in key state variables in some applications. This oscillatory behavior becomes severe especially as the mesh size is reduced (Frepoli et al., 2000).

When the flow is expected to vary slowly with time and the mesh size is small, the fully-implicit method is more attractive. CATHARE is among the thermal-hydraulics code based on the fully-implicit method (Bestion, 1990). RETRAN (Katsma et al., 1985) was originally based on a semi-implicit method. Then a two-step solution procedure was used for the basic three-equation (continuity, energy, momentum) HEM model. This procedure eliminated CFL limitations on the time step size but it failed when the model was extended to the four-equation model (additional slip equation). These issues were resolved as a 'partial' fully-implicit method was implemented in

more recent versions of RETRAN-02 (Katsma et al., 1985). The code is only fully-implicit with respect to mass, energy and momentum flux terms while heat transfer and friction coefficients are still evaluated explicitly. VIPRE-02 (Kelly et al., 1992) is a two-fluid thermal-hydraulic code used to simulate steady-state conditions and operational transients in Light Water Reactor (LWR) cores and vessels. The code is based on a fully-implicit scheme and an iterative process is used to advance in time, the solution of all six conservation equations. An inner iteration loop is used to solve the continuity equations first and an outer iteration loop proceeds to the solution of the energy and momentum equations. The VIPRE-02 code developers claimed that by quickly eliminating the convergence error from the continuity equations and obtaining a better estimate of the flow field for the energy and momentum equations, the overall solution converge more efficiently.

On a different front the Piecewise Linear Interpolation Method (PLIM) was proposed by Rajamaki (1996) to eliminate excessive errors, numerical diffusion and dispersion during the solution of the time-dependent one-dimensional two-phase flow equations in network geometry. The method originates from the consideration that different type of disturbances (pressure, void fraction, etc.) propagates at different characteristic velocities. Rajamaki (1996) indicated that an algorithm, which disregards the characteristic velocities, is not applicable to general, accurate calculation of flow phenomena. The PLIM method is also described as a shape-preserving characteristic method. The fundamental assumption is that the equations form an initial value problem with respect to time (hyperbolic equations).

Based on similar considerations the fully-implicit method was selected for the development of the computational model described in this paper. The model is based on a fine hydraulic mesh used to describe the complex phenomena occurring in the quench front and froth region in a reactor core during the reflood phase of a postulated LOCA accident. At the quench front region the thermal-hydraulic parameters experience a sharp axial variation. Different heat transfer regimes occur simultaneously over a short distance. The large amount of steam generated in proximity of the quench front causes a large axial variation in the void fraction. The steam flow entrains liquid droplets and the two-phase flow is rather complex. A three-field model, which distinguishes between the entrained portion of the liquid (droplets) and the continuous field, is necessary to fully describe the flow in that region. On the other hand current models are too coarse for a mechanistic description of the phenomena. The resolution of the axial variations on a small space scale requires a very fine hydraulic mesh.

A complete fully-implicit implementation is more involved and practicable only for one-dimensional two-phase problems. For three-dimensional two-phase problems the implementation of a fully-implicit scheme is still possible but it requires special techniques such as fractional time steps or direction splitting. The most widely used one-dimensional fully-implicit thermal-hydraulics model is CATHARE (Bestion, 1990). Unlike the semi-implicit scheme, in the fully-implicit method the new time value of the phasic velocities is evaluated at several nodes. A global Newton method is required to solve simultaneously momentum, mass and energy equations.

The attractiveness of the fully-implicit scheme is that for a single-phase flow the fully-implicit numerical scheme is unconditionally stable. For a given node size the time step size can significantly exceed the material Courant limit, especially when the flow conditions are slowly changing with time.

For extremely fine mesh, there are other issues which complicate the two-phase problem. The first one is that the derivation of the two-fluid equations and constitutive relations is based on some space and time averaging hypothesis (Ishii and Mishima, 1982). These hypotheses start to fail for an extremely fine mesh. This determines a lower bound to the minimum size of the mesh that can be employed. For instance the description of the bubbly flow model based on space averaged macroscopic quantities with a mesh size smaller than the bubble itself is inconsistent.

The other aspect is that the single-pressure two-phase flow model is known to be mathematically ill-posed (Gidaspow, 1974; Ramshaw and Trapp, 1978; Lyczkowski, 1980) because of the existence of complex characteristics. Lyczkowski et al. (1978) showed theoretically that in this case the fully-implicit method, which is unconditionally stable for hyperbolic systems, is unstable.

Several models have been proposed by researchers to render the characteristics of the two-phase

single-pressure model real (Ramshaw and Trapp, 1978; Ransom and Hicks, 1984; Arai, 1980; Stuhmiller, 1977; Banerjee and Chan, 1980; Lahey et al., 1980; No and Kazimi, 1985). These models suggest inclusion of regularization terms in the conservation equation based on consideration of virtual mass, interfacial pressure, artificial viscosity, etc. Some of these techniques have been included in different thermal-hydraulic codes such as RELAP5 (Shieh et al., 1994) and CATHARE (Bestion, 1990). More recent works investigate the role of the momentum flux parameters in determining the stability by looking at the effect of void fractions and velocity profiles (Song and Ishii, 2001a,b). In their work Song and Ishii showed that the compressible one-dimensional two-fluid model is stable for the whole range of flow regimes by use of appropriate momentum flux parameters. The applicable range of all these models is still limited and it is recognized that, with or without regularization terms, practicable solutions can be obtained despite the ill-posed-ness of the two-fluid problem. This is still not clear but one of the reasons is the dumping of short wave-length instabilities exerted by the finite difference equations (Krishnamurthy and Ransom, 1992; Pokharna et al., 1997). For the aforementioned reasons, it was decided not to apply these techniques to the fully-implicit method presented in this paper hoping that the stabilizer effect offered by the finite difference scheme will enable us to obtain a well-behaved solution.

Nevertheless the intricacies of the solution of the two-fluid single-pressure problem have indeed an unstable nature because of the non-linearities. The development of various numerical techniques applies at different extents to all differential approaches, i.e. semi-implicit or fully-implicit. The implementation of these techniques is very time consuming and the most challenging task for the code developer. The literature on these issues generally concentrates on the theoretical aspects of the numerical method but available information on the problems encountered during the implementation of such methods is scarce. The reason is that many of these methods are somewhat empirical and are developed as a result of a long and tedious trial and error process. Also these methods often lack in generality and a particular method that works fine under certain conditions, can lead to failure for different conditions.

2. Governing equations

The present model describes the one-dimensional two-phase flow based on the three-field description where the liquid phase is divided into the continuous field and the dispersed field. The use of the three-field model is particularly useful in describing the thermal-hydraulics of a reactor core during a hypothetical Large Break Loss of Coolant Accident (LBLOCA). In addition the model solves the heat conduction and the heat transfer from the wall to the fluid.

The three-field formulation of the two-phase flow is a straightforward extension of the two-fluid single-pressure model (Lahey and Drew, 1990; Ishii and Mishima, 1982). The fields included are vapor, continuous liquid, and entrained liquid. The one-dimensional fluid flow is governed by eight equations: three mass conservation equations, two energy equations and three momentum conservation equations. The use of two energy equations instead of three is justified by assuming that the enthalpy of the continuous liquid field is equal to the enthalpy of the dispersed liquid field. This is a good approximation for most of the applications of interest. The three mass conservation equations are:

$$\frac{\partial(\alpha_v\rho_v)}{\partial t} = -\frac{\partial(\alpha_v\rho_v u_v)}{\partial x} + \Gamma''' \tag{1}$$

$$\frac{\partial(\alpha_l\rho_l)}{\partial t} = -\frac{\partial(\alpha_l\rho_l u_l)}{\partial x} - (1-\eta)\Gamma''' + S_D''' - S_E''' \tag{2}$$

$$\frac{\partial(\alpha_e\rho_l)}{\partial t} = -\frac{\partial(\alpha_e\rho_l u_e)}{\partial x} - \eta\Gamma''' - S_D''' + S_E''' \tag{3}$$

The coefficient η in the previous equations is the fraction of vapor generated by droplets. The two conservation of energy equations are:

$$\frac{\partial(\alpha_v\rho_v h_v)}{\partial t} = -\frac{\partial(\alpha_v\rho_v u_v h_v)}{\partial x} + \Gamma''' h_g + q_{iv} + Q_{wv} + \alpha_v\frac{\partial P}{\partial t} \tag{4}$$

$$\frac{\partial((1-\alpha_v)\rho_l h_l)}{\partial t} = -\frac{\partial((\alpha_l u_l + \alpha_e u_e)\rho_l h_l)}{\partial x} - \Gamma''' h_f + q_{il} + Q_{wl} + (1-\alpha_v)\frac{\partial P}{\partial t} \tag{5}$$

The three momentum conservation equations are written in the non-conservative form as:

$$\alpha_v\rho_v\frac{\partial u_v}{\partial t} = -\alpha_v\rho_v u_v\frac{\partial u_v}{\partial x} - \alpha_v\rho_v g - \alpha_v\frac{\partial P}{\partial x} - \tau_{wv} - \tau_{i,vl} - \tau_{i,ve} - \Gamma'''_E(u_v - (1-\eta)u_l - \eta u_e) \quad (6)$$

$$\alpha_l\rho_l\frac{\partial u_l}{\partial t} = -\alpha_l\rho_l u_l\frac{\partial u_l}{\partial x} - \alpha_l\rho_l g - \alpha_l\frac{\partial P}{\partial x} - \tau_{wl} + \tau_{i,vl} + (1-\eta)\Gamma'''_C(u_v - u_l) + S'''_D(u_e - u_l) \quad (7)$$

$$\alpha_e\rho_l\frac{\partial u_e}{\partial t} = -\alpha_e\rho_l u_e\frac{\partial u_e}{\partial x} - \alpha_e\rho_l g - \alpha_e\frac{\partial P}{\partial x} + \tau_{i,ve} + \eta\Gamma'''_C(u_v - u_e) - S'''_E(u_e - u_l) \quad (8)$$

where S'''_E and Γ'''_C are, respectively, the vapor source contributions due to evaporation of the liquid and due to condensation of the steam. The net vapor generation source term Γ''' is given by the difference of the two contributions:

$$\Gamma''' = \Gamma'''_E - \Gamma'''_C \quad (9)$$

The models and correlations, which are used to define the closure relationships for the fluid flow equations, are based on the COBRA-TF heat transfer and fluid packages (Paik et al., 1985; Thurgood and George, 1983).

In addition to the fluid flow equation, for the droplet field an interfacial area transport equation is used to determine the interfacial area of the liquid dispersed field:

$$\frac{\partial A'''_{i,d}}{\partial t} + \frac{\partial}{\partial x}(A'''_{i,d}u_e) = \left(\frac{\partial A'''_{i,d}}{\partial t}\right)_E + \left(\frac{\partial A'''_{i,d}}{\partial t}\right)_\Gamma \quad (10)$$

Eq. (10) states that the total time derivative of the interfacial area concentration is equal to the sum of two contributions: the change of interfacial area due to the entrainment of droplets and the change due to the evaporation of the droplets. Eq. (10) does not include the volume expansion term as mentioned by Hibiki and Ishii's paper (2001). Here the interfacial area concentration transport equation is only used to model the droplet field evolution. Since the liquid is almost incompressible, the volume expansion term was neglected and omitted in Eq. (10).

The droplet diameter is related to the interfacial area concentration by the following equation:

$$D_d = \frac{6\alpha_e}{A'''_{i,d}} \quad (11)$$

To complete the set, a two-dimensional heat conduction model is used to calculate the heat transfer within heated structures and the heat transfer from the wall surface to the fluid.

3. Finite volume equations

The finite difference equations are obtained from the typical staggered-mesh–finite-volume scheme where the velocities are obtained at the mesh cell faces and the state variables, such as pressure, density, enthalpy, and void fraction, are obtained at the cell center.

The finite volume equations are obtained by integrating the conservation (PDE) equations over the control volume. In particular this model was originally developed to solve the coupled heat transfer and fluid flow problem on fine moving mesh (Frepoli et al., 2000). The PDE equations were integrated over a moving, non-deforming control volume. The moving grid is outside the scope of this paper and for sake of clarity the equations are here written for a fixed grid. The finite volume conservation equations for the vapor field are:

Conservation of vapor mass:

$$\frac{(\alpha_v\rho_v)_j^{n+1} - (\alpha_v\rho_v)_j^n}{\Delta t}A_j\Delta x_j = A_{j-(1/2)}(\alpha_v\rho_v)_b^{n+1}(u_v)_{(j-1/2)}^{n+1} - A_{j+(1/2)}(\alpha_v\rho_v)_a^{n+1}(u_v)_{j+(1/2)}^{n+1} + \Gamma_j^{n+1} \quad (12)$$

Conservation of vapor energy:

$$\frac{(\alpha_v\rho_v h_v)_j^{n+1} - (\alpha_v\rho_v h_v)_j^n}{\Delta t}A_j\Delta x_j = A_{j-(1/2)}(\alpha_v\rho_v h_v)_b^{n+1}(u_v)_{j-(1/2)}^{n+1} - A_{j+(1/2)}(\alpha_v\rho_v h_v)_a^{n+1}(u_v)_{j+(1/2)}^{n+1} + \Gamma_j^{n+1}h_g + (q_{iv})_j^{n+1} + (Q_{wv})_j^{n+1} + (\alpha_v)_j^{n+1}A_j\left(\frac{P_j^{n+1} - P_j^n}{\Delta t}\Delta x_j\right) \quad (13)$$

Conservation of vapor momentum:

$$
\begin{aligned}
&(\alpha_v\rho_v)^{n+1}_{j+(1/2)}\frac{(u_v)^{n+1}_{j+(1/2)}-(u_v)^{n}_{j+(1/2)}}{\Delta t}A_{j+(1/2)}\Delta x_{j+(1/2)}\\
&\quad=A_j(\alpha_v\rho_v u_v)^{n+1}_{j+(1/2)}((u_v)^{n+1}_{b}-(u_v)^{n+1}_{a})-g(\alpha_v\rho_v)^{n+1}_{j+(1/2)}A_{j+(1/2)}\Delta x_{j+(1/2)}\\
&\qquad-(\alpha_v)^{n+1}_{j+(1/2)}(P^{n+1}_{j+1}-P^{n+1}_{j})A_{j+(1/2)}-(\tau_w)^{n+1}_{j+(1/2)}-(\tau_{i,vl})^{n+1}_{j+(1/2)}-(\tau_{1,ve})^{n+1}_{j+(1/2)}\\
&\qquad-(\Gamma_E)^{n+1}_{j+(1/2)}((u_v)^{n+1}_{j+(1/2)}-(1-\eta^{n+1}_{j+(1/2)})(u_l)^{n+1}_{j+(1/2)}-\eta^{n+1}_{j+(1/2)}(u_e)^{n+1}_{j+(1/2)})
\end{aligned}
\tag{14}
$$

Similar equations apply to the other fields. The scalar quantities at the boundary of the continuity cell are evaluated with a simple average as follows:

$$
\begin{aligned}
(\alpha_k)_{j+(1/2)}&=\frac{(\alpha_k)_j+(\alpha_k)_{j+1}}{2}\\
(\rho_k)_{j+(1/2)}&=\frac{(\rho_k)_j+(\rho_k)_{j+1}}{2}
\end{aligned}
\tag{15}
$$

The suffix ‘a’ and ‘b’ defines quantities that are evaluated, respectively, at the upper and lower boundary of the cell based on the donor scheme. For example, the velocities at the boundary of the momentum cell are evaluated as follows:

$$
\begin{aligned}
(u_k)_b=\frac{1}{2}\Bigg[&((u_k)_{j-(1/2)}+(u_k)_{j+(1/2)})\\
&+\frac{(u_k)_{j+(1/2)}}{|(u_k)_{j+(1/2)}|}((u_k)_{j-(1/2)}+(u_k)_{j+(1/2)})\Bigg]
\end{aligned}
\tag{16}
$$

The source of entrainment and de-entrainment are calculated explicitly based on the ‘old’ time fluid conditions. The interfacial area concentration transport Eq. (10) for the droplet field is integrated in space with the FVM and explicit in time. As a result the new value of the interfacial area concentration is determined by the following equation:

$$
\begin{aligned}
(A'''_{i,d})^{n+1}_j=(A'''_{i,d})^{n}_j&\left(1-\frac{\eta\Gamma_j\Delta t_i}{(\rho_l)_j(\alpha_e)_j}\right)^{2/3}\\
&+\Bigg\{((A'''_{i,d})^{n}_b(u_e)_{j-(1/2)}A_{j-(1/2)}\\
&-(A'''_{i,d})^{n}_a(u_e)_{j+(1/2)}A_{j+(1/2)})\\
&+\left(\left(\frac{\partial A'''_{i,d}}{\partial t}\right)_E\right)^{n}_j\Bigg\}\frac{\Delta t_i}{\Delta x A_j}
\end{aligned}
\tag{17}
$$

where the first term on the R.H.S. is the change of surface area as result of the evaporation and the 2/3 exponent comes from the relation between volume and surface assuming spherical droplets. Note that, in order to prevent the calculation of the flow solution from being limited by the Courant material limit, the interfacial area concentration transport equation is integrated in time using a time step size Δt_i which is a fraction of the time step size used for the flow solution. As a result the solution of the interfacial area concentration is decoupled from the fluid flow solution.

As with the fluid flow equations, the heat conduction equation is integrated using a FVM. The solution of the heat conduction is based on the ADI method (Tannehill et al., 1997). The ADI method is unconditionally stable and for a two-dimensional problem the solution matrix is tridiagonal. Therefore the matrix inversion can be performed with limited effort by using the Thomas formula (Tannehill et al., 1997). The heat transfer from the wall to the fluid is implicitly coupled with a method similar to the one included in RELAP5 (RELAP5 Code Development Team, 1995a,b). The full derivation of these equations can be also found in Frepoli (2001).

4. Solution of the equation set

The previous set of non-linear equations is solved with the Newton iterative method (Golub and Ortega, 1993; Dennis and Schnabel, 1996). The Newton’s method is a powerful technique for solving systems on non-linear equations. The set of equations is written as:

$$
\bar{F}(\bar{x})=\left[f_1(\bar{x}),\,f_2(\bar{x}),\ldots,f_N(\bar{x})\right]^{T}=0
\tag{18}
$$

where

$$
\bar{x}=[x_1,x_2,\ldots,x_N]^{T}
\tag{19}
$$

The Newton's method is an iterative method. From a first order Taylor's expansion of $\bar{F}(\bar{x}^{m+1})$ about the approximate solution at the iteration 'm' $\bar{x}^m$ we have:

$$\bar{F}(\bar{x}^{m+1}) \approx \bar{F}(\bar{x}^m) + \frac{\partial \bar{F}}{\partial \bar{x}^m}\delta\bar{x}^m = \bar{F}(\bar{x}^m) + \bar{\bar{J}}^m \delta\bar{x}^m \tag{20}$$

where $\bar{\bar{J}}^m$ is the Jacobian matrix. The Newton's method seeks the solution update $\delta\bar{x}^m$ that drives $\bar{F}(\bar{x}^{m+1})$ to zero. This translates in solving the following linear system of equations:

$$\bar{\bar{J}}^m \delta\bar{x}^m = -\bar{F}(\bar{x}^m) \tag{21}$$

The new solution vector is then updated as follows:

$$\bar{x}^{m+1} = \bar{x}^{m+1} + \delta\bar{x}^m \tag{22}$$

The vector $\bar{F}(\bar{x}^m)$ is also called vector of residuals. The iteration is continued until the residuals are below some tolerance level.

In particular in our one-dimensional problem, for each node there are nine FDE Equations with nine independent variables. The solution vector is in this case:

$$\begin{aligned}\bar{x} = [&P_2, \alpha_{v_2}, \alpha_{e_2}, h_{v_2}, h_{l_2}, u_{v_{3/2}}, u_{l_{3/2}}, u_{e_{3/2}},\\ &\times T_{w_{nr,2}}, \ldots, P_{nx}, \alpha_{v_{nx}}, \alpha_{e_{nx}}, h_{v_{nx}}, h_{l_{nx}},\\ &\times (u_v)_{nx+(1/2)}, (u_l)_{nx+(1/2)}, (u_e)_{nx+(3/2)}, T_{w_{nr,nx}}]^T\end{aligned} \tag{23}$$

The selection of the independent variables varies from code to code. In RELAP5, the internal energy is used instead of the enthalpy. In COBRA-TF the product of enthalpy and void fraction for each phase is selected as independent variable. In TRAC-PD2 the phasic temperatures are used instead of enthalpies. The use of the temperature is more natural since the steam properties (density, viscosity, etc.) are typically expressed as function of temperature. The use of the product of enthalpy and void fraction is convenient during the analytical derivation of the Jacobian. In general there are pros and cons for each selection and the trade off is unclear. Often the developer makes the selection based more on historical reasons. The numerical model is then adapted to the selection.

For a given set of non-linear equations and the corresponding independent variables, a key-step in the Newton method is represented by the evaluation of the Jacobian. With the semi-implicit scheme, the momentum equation can be de-coupled from the mass and energy equations. The problem can then be reduced to a set of pressure equation and the elements of the Jacobian are typically evaluated with analytical expressions.

The evaluation of the Jacobian elements is a cumbersome task for the fully-implicit methods, especially for three-dimensional problems or cases like this one with many equations involved. In the fully-implicit method the velocity must be solved at several nodes and momentum, mass and energy equations need to be solved simultaneously.

In the numerical model presented in this paper the coefficients of the Jacobian matrix are evaluated numerically with a perturbation technique (McHugh, 1995) which is further discussed in Section 6. The numerical evaluation of the Jacobian provides more flexibility to the code developer. It is possible to explore different numerical schemes or add new equations with relative ease. It also resulted in a more reliable program, since analytic evaluation of the Jacobian terms is one of the most difficult and error prone tasks during the implementation of a fully-implicit scheme for multiphase flow.

4.1. Special treatment for the single-phase flow regime

One of the difficulties encountered in modeling two-phase flow is the treatment of the transition from the two-phase to the single-phase regime. The previous equation set becomes singular when one field is missing (single-phase liquid or single-phase vapor).

In other computer codes (for example in RELAP5, COBRA-TF and CATHARE) the singularity of the solution matrix is prevented from occurring by limiting the minimum value of the void fraction to a very small value but greater than zero. Typically the interfacial drag coefficients are set to very large value as the flow approaches single-phase. This forces a mechanical equilibrium between the phases. The method prevents the singularity from occurring, however, if not handled properly, it introduces some artificial momentum source terms in the equation of the dominant phase.

There are also complications when the previous technique is applied in combination with a fully-implicit scheme. These are related to the fact

that the void fraction is also an independent variable. Early attempts by the authors to bound the void fraction during the Newton iterations encountered the convergence difficulty at the transition point between single-phase and two-phase.

In our current numerical model, the singularity was precluded without adding any artificial limitations on void fraction or non-physical interfacial drag terms. Governing equations are selected in a given volume based on the predicted void fractions. The two-phase equations described above are used when appropriate. However, when contents of a cell volume are all liquid or all vapor, single-phase equations are used. For example, if the flow is expected to be single-phase vapor, the mass and energy conservation of the vapor field are replaced by mixture mass and energy equations and other equations are used for the missing field. The mass and energy conservation equations for the single-phase vapor are:

$$\frac{\partial}{\partial t}(\alpha_v\rho_v + (1-\alpha_v)\rho_l) = -\frac{\partial}{\partial x}(\alpha_v\rho_v u_v + \alpha_l\rho_l u_l + \alpha_e\rho_l u_e) \quad (24)$$

$$\alpha_l = 0 \quad (25)$$

$$\alpha_e = 0 \quad (26)$$

$$\frac{\partial}{\partial t}(\alpha_v\rho_v h_v + (1-\alpha_v)\rho_l h_l) = -\frac{\partial}{\partial x}(\alpha_v\rho_v u_v h_v + (\alpha_l u_l + \alpha_e u_e)\rho_l h_l) + Q_{wv} + Q_{wl} + \frac{\partial P}{\partial t} \quad (27)$$

$$h_l = h_f \quad (28)$$

The momentum equations are modified by eliminating the terms related to the field that is missing from the equation of the dominant phase. Then the momentum equation of the missing field is modified such that the equation is not singular. For instance, the three momentum equations for a flow with no continuous liquid are:

$$\alpha_v\rho_v\frac{\partial u_v}{\partial t} = -\alpha_v\rho_v u_v\frac{\partial u_v}{\partial x} - \alpha_v\rho_v g - \alpha_v\frac{\partial P}{\partial x} - \tau_w - \tau_{i,ve} - \Gamma'''_E(u_v - u_e) \quad (29)$$

$$\alpha_{l,\min}\rho_l\frac{\partial u_l}{\partial t} = -\alpha_{l,\min}\rho_l u_l\frac{\partial u_l}{\partial x} - \alpha_{l,\min}\rho_l g - \alpha_{l,\min}\frac{\partial P}{\partial x} - \tau_{wl} + \tau_{i,vl} \quad (30)$$

$$\alpha_e\rho_l\frac{\partial u_e}{\partial t} = -\alpha_e\rho_l u_e\frac{\partial u_e}{\partial x} - \alpha_e\rho_l g - \alpha_e\frac{\partial P}{\partial x} + \tau_{i,ve} + \eta\Gamma'''_C(u_v - u_e) \quad (31)$$

The minimum value $\alpha_{l,\min}$ is set to 10^{-6}.

In this case, as the flow approaches single-phase the interfacial drag coefficient used in the momentum equation of the missing field is calculated based on a physical approach. For instance if the continuous liquid field becomes depleted, it is effectively assumed that a single drop, whose diameter D_{SD} is calculated as follows, carries all residual liquid:

$$D_{SD} = \left(\frac{6}{\pi}\alpha_{l,\min}V_{cell}\right) \quad (32)$$

The interfacial drag coefficient is then calculated as:

$$K_{vl} = \frac{3}{4}C_D\frac{\rho_v\alpha_{l,\min}V_{cell}}{D_{SD}} \quad (33)$$

The single drop drag coefficient is assumed for simplicity $C_D = 0.5$.

A similar approach is used when the entrained droplet field becomes depleted. The residual dispersed field is assumed to be distributed among a population of droplets with a minimum diameter. The minimum diameter is set equal to:

$$D_{\min} = 10^{-6}\,\text{m} \quad (34)$$

The interfacial drag between the vapor and the dispersed field is calculated as:

$$K_{vl} = \frac{3}{4}C_D\frac{\rho_v\alpha_{e,\min}V_{cell}}{D_{\min}} \quad (35)$$

The previous interfacial drag term is removed from the momentum equation of the dominant phase (i.e. the vapor field in this case) and is applied only to the momentum equation of the vanishing field. In other words at the limit of single-phase the momentum equation of the dominant field is de-coupled from the momentum equation of the vanishing field. The equation set is mathematically consistent with the single-phase flow regime and the solution matrix is non-singular.

A similar method is used to define the momentum equations when the vapor field vanishes. This method

ensures that the momentum equation of the missing field is decoupled from the other two momentum equations. As a result the model does not introduce artificial source terms in the momentum equation of the dominant field and provides a continuous transition from single-phase to two-phase flow regime.

This new approach represents a significant improvement over the current method of simply forcing the interfacial transfer terms to force one phase to the other. Main advantages are the following:

1. It addresses the singularity of the solution matrix as the flow approaches single-phase flow conditions.
2. It ensures a more rigorous mass conservation at the limit of single-phase flow whereas other methods can lead to solutions with negative void fraction values.
3. At the limit, the phasic velocities solution for the depleted field obtained with the single-phase equation set is consistent with the velocities that are calculated using the two-phase equation set.
4. Excessive condensation of steam at the limit of single-phase liquid flow or excessive evaporation of liquid at the limit of single-phase vapor is prevented from occurring. The switch to the single-phase equation set is mathematically equivalent to condensing or evaporating just the residual steam or liquid which is present in the cell.

However it has to be noted that this method is still susceptible to water packing and requires special corrections (Mahaffy and Liles, 1983) or good level tracking (Aktas and Mahaffy, 1996), which are typical of other thermal-hydraulic models.

The equation set to be used at a given time step in a given cell is selected at the beginning of the time step by obtaining a predicted value of the void fraction of each phase. The predicted value is obtained by solving for the total liquid fraction an explicit mass conservation equation:

$$\begin{aligned}(\alpha^*_{\mathrm{liq}})_j &= (\alpha^*_{\mathrm{l}})_j + (\alpha^*_{\mathrm{e}})_j \\ &= (\alpha^n_{\mathrm{l}})_j + (\alpha^n_{\mathrm{e}})_j + \frac{\Delta t}{(\rho^n_{\mathrm{l}})_j A_j \Delta x_j}(\dot{m}^n_{\mathrm{liq},\,j-(1/2)} \\ &\quad -\dot{m}^n_{\mathrm{liq},\,j+(1/2)} - \Gamma^n_j) \end{aligned} \tag{36}$$

If the predicted liquid fraction is less than 10^{-6} then the flow for that node is flagged single-phase vapor and similarly if the predicted liquid fraction is greater than 0.999999 the flow is flagged single-phase liquid.

The predicted void fraction is also used to determine a better initial guess for the Newton iteration. For instance the new guess for the void fraction is calculated as follows:

$$\begin{aligned}\alpha^*_{\mathrm{v},\,j} &= (\alpha^n_{\mathrm{v}})_j + \frac{\Delta t}{(\rho_{\mathrm{v}})^n_j A_j \Delta x_j}(\dot{m}^n_{\mathrm{v},\,j-(1/2)} \\ &\quad -\dot{m}^n_{v,\,j+(1/2)} + \Gamma^n_j) \end{aligned} \tag{37}$$

$$\begin{aligned}\alpha^*_{\mathrm{e},\,j} &= (\alpha^n_{\mathrm{e}})_j + \frac{\Delta t}{(\rho_{\mathrm{l}})^n_j A_j \Delta x_j}(\dot{m}^n_{\mathrm{e},\,j-(1/2)} - \dot{m}^n_{\mathrm{v},\,j+(1/2)} \\ &\quad +(S_{\mathrm{E}})^n_j - (S_{\mathrm{DE}})^n_j - \eta_j \Gamma^n_j) \end{aligned} \tag{38}$$

4.2. Convergence criteria

The convergence is checked looking at the variables' updates for each Newton iteration and convergence is reached when the variables' increments satisfy the following criteria:

$$\begin{aligned}&\max\left(\frac{\Delta P_i}{P_i}\right) \le \varepsilon_n \\ &\max\left(\frac{\Delta\alpha_{\mathrm{v}}}{\max(10^{-6}, \min(\alpha_{\mathrm{v}}, 1-\alpha_{\mathrm{v}}))}\right)_i \le 100\varepsilon_n \\ &\max\left(\frac{\Delta\alpha_e}{\max(10^{-6}, \alpha_{\mathrm{e}})}\right)_i \le 100\varepsilon_n \\ &\max\left(\frac{\Delta H_{\mathrm{v}}}{H_{\mathrm{v}}}\right)_i \le \varepsilon_n \qquad \max\left(\frac{\Delta H_{\mathrm{l}}}{H_{\mathrm{l}}}\right)_i \le \varepsilon_n \end{aligned} \tag{39}$$

The selected value for the tolerance ε_n is 10^{-4}. The convergence criteria on the void fraction is similar to the one used in the one-dimensional module of CATHARE code (Bestion, 1990). However a more stringent convergence criteria than the one used in the CATHARE code is used for the pressure and the enthalpy. A looser criterion on mass and energy was found to cause the calculation to diverge under certain conditions.

Divergence is checked if the variables' increments between two Newton iterations are too large or if the value of the new variables exceeds defined upper or lower bounds on pressure and enthalpy. Pressure and enthalpy are used to calculate the water properties and these variables needed to be bounded to ensure that their value is always inside the interpolation region of

the steam tables used within the code. In the case of divergence, current variables are not updated and the time step is repeated with a smaller time step size. This procedure is sometimes called backup.

The user sets the minimum and maximum allowed time steps via input. If internal time step control requires a time step size below the user specified minimum, the calculation is stopped. Typically, for the calculations presented here the minimum time step is in the 10^{-7} to 10^{-5} s range and the maximum time step is equal to 0.1 s. Note that in a thermal-hydraulic calculation, if time step size goes below 10^{-5} something is seriously wrong and the code or problem specification needs to be examined. Between these limits, the time step is automatically controlled by the code. The value of the $(n + 1)$th time step is determined by the following equation:

$$\Delta t^{n+1} = k\Delta t^{n} \tag{40}$$

where k depends on n_1, the number of iterations at the nth time step, and n_2, the number of iterations at $(n - 1)$th time step as follows:

$$k = \begin{cases} 0.5 & \text{if } n_1 \geq 8 \\ 1.1 & \text{if } n_1 \leq 3 \text{ and } n_2 \leq 3 \\ 1.0 & \text{otherwise} \end{cases} \tag{41}$$

5. Numerical test models

The computational model was tested against some numerical test benchmarks. Test Problem 1 (Fig. 1) is a modified version of the numerical benchmark NBT2.3 reported in Hewitt et al. (1992). The same geometry, initial and boundary conditions are used in the test as the numerical benchmark. Subcooled water is injected at a constant rate from the bottom of a volume initially filled with superheated steam. However, in the Test Problem 1, the interfacial heat transfer is turned-off such that the hydraulic behavior can be isolated. Test Problem 2 is the same as NBT2.3: the interfacial heat transfer is activated and the effect of condensation is included.

Test Problem 3 was taken from Aktas and Mahaffy (1996). The schematic diagram of this test is shown in Fig. 2. The original test problem was based on air–water flow. Test Problem 3 is based on the same pressure, temperature conditions but air is replaced with steam since air properties are not included in the current model. However the interfacial heat transfer is turned-off such that the predictions can be compared to the results presented in the original paper. During the first 10 s of the transient, a steady-state is established

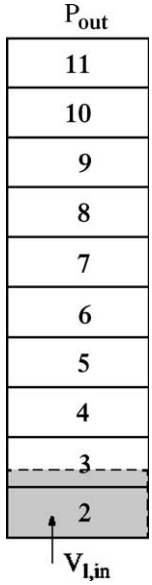

Fig. 1. Schematic and noding diagram Test Problems 1 and 2.

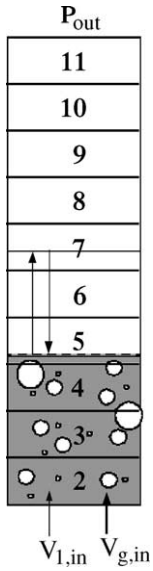

Fig. 2. Schematic and noding diagram Test Problem 3.

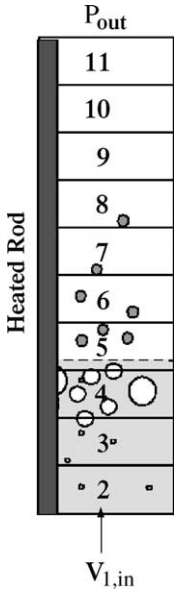

Fig. 3. Schematic and noding diagram Test Problem 4.

by injecting a constant flow rate of steam in a stagnant pool of water. The steady-state mixture level is calculated in node 5 (Fig. 2). At 10 s water starts to be injected at the velocity 5 cm/s for 5 s. At 15 s the liquid flow rate is reversed and the inlet liquid velocity is set to −5 cm/s for another 5 s. As a result between 10 and 20 s (transient portion) the mixture level crosses two cell boundaries in both directions as depicted in Fig. 2.

The two-phase flow computational model discussed in this paper was originally developed to model details (with a fine hydraulic mesh) of the complex three-field flow and heat transfer in proximity of the quench front of a reactor core during the reflood phase of LBLOCA transient. Test Problem 4 was designed to test the model for conditions that are similar to the one expected during reflood. The schematic of the test problem is shown in Fig. 3. The geometry and conditions correspond to one of the FLECHT-SEASET tests (Lee et al., 1981; Loftus et al., 1980). The Full Length Emergency Core Heat Transfer–System Effects And Separate Effect Tests (FLECHT–SEASET) test program was performed during the 1980s to simulate the reflood in a typical PWR geometry. The test facility is a full-length 161-rod bundle, which has the same geometry, rod diameter and pitch, of a typical Westinghouse PWR core with 17 × 17 fuel rod arrays. Among the FLECHT-SEASET experiments, the test Run 31504, which is characterized by a constant flooding rate of 2.44 cm/s, was the test selected for this analysis. The model describes the first 0.5 m vertical section of the bundle. A linear temperature profile is pre-assigned to the rod where wall temperature varies from 204 °C (400 °F) at the bottom to 427 °C (800 °F) at the top of the model. Pressure is set to a constant value of 272 kPa (40 psia) at the top of the model. The volume is filled initially with saturated steam. The transient begins as subcooled water at 98 °C is injected at the bottom of the bundle at a constant rate of 2.44 cm/s. As the transient proceeds, the rod is quenched, steam is generated and liquid droplets are entrained creating a rather complex thermal-hydraulic problem to solve. A mesh with 10 equal nodes (5 cm each) is used to subdivide the vertical length of both the flow channel and the rod. The rod component is also subdivided in the radial direction in 10 conduction nodes.

6. Coding issues and assessment of the fully-implicit model

The two-fluid single-pressure problem has an intrinsic unstable nature associated with the ill-posed-ness. As already discussed in Section 1, these type of instabilities are generally dumped by the finite difference approximation of the equations and become an issue only for very small mesh size which are not considered here. Moreover at those extreme small mesh sizes, even the averaging assumptions, which are at the basis of the two-fluid model, tend to fail (Stewart and Wendroff, 1984).

Nevertheless, beyond the previous considerations, in order to achieve a robust solution of any coupled non-linear equations it is necessary to develop various numerical techniques. The attempt of this section is to capture as much as possible, the lessons learned during the development and coding of the present fully-implicit two-phase model. The analysis presented here should provide some insights and guidelines for future development of this model or similar models. Several numerical studies have been conducted to develop and refine the techniques. These studies were based on the test problems described

in the previous section. Since the code was designed to solve the complex phenomena in the quench front and froth region during core reflood, Test Problem 4 was used as the base case in most of the numerical studies that follow. The other test problems were used to separately study some particular phenomenon.

6.1. Convergence criteria

The most rigorous convergence criteria for a Newton method examine the vector of residuals and then compare the residuals at each iteration against a small tolerance ε_n. More common convergence criteria are based upon the relative update of each independent variable and assume convergence when the relative update is below a small tolerance.

For single-phase, compressible flow calculations McHugh (1995) suggested a combination of these two methods. In his work the convergence is assumed when:

$$\max\left(\frac{|\delta x_i|}{\max(|x_i|, 1)}\right) \leq \varepsilon_n = 10^{-6} \tag{42}$$

and

$$||\bar{F}(\bar{x})|| \leq \varepsilon_n = 10^{-6} \tag{43}$$

where $\bar{x}$ is the vector of independent variables, δx_i is the update to the independent variable x_i and $||\bar{F}(\bar{x})||$ is the norm of the vector of residuals. The first criteria determine the required accuracy of the update and the second criteria establish a minimum value for the residuals. This method was developed for the steady-state solution of single-phase low Mach

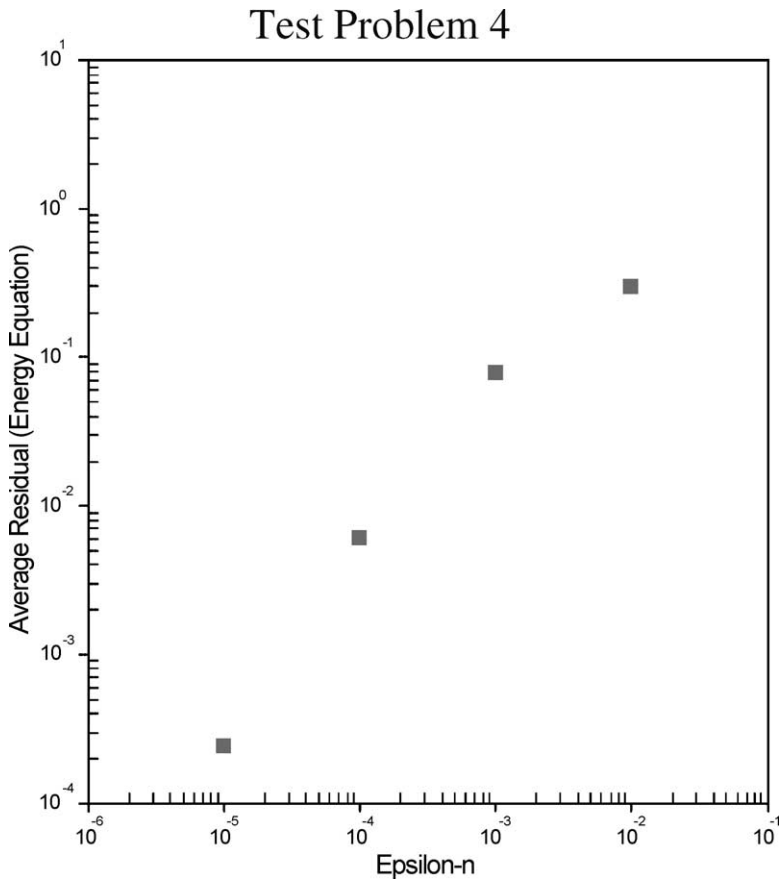

Fig. 4. Effect of the convergence tolerance coefficient (ε_n) on the magnitude of the average residual.

number compressible fluid flow and heat transfer problems. The same method was attempted in an early version of this two-phase transient model. It was found that for a transient calculation the previous criteria is too stringent and the convergence criteria is impractical. If ε_n is reduced to 10^{-4}, the McHugh method is workable and can keep residuals at a relative low value. However the second requirement of the McHugh method is still quite severe and can be achieved only by significantly reducing the time step size. The other problem of the McHugh method, when applied to the two-phase problem is that the second requirement does not distinguish between different equations whose residual has a different magnitude but a similar relative importance. More attractive criteria should be based on appropriate scaling of variables. The convergence method that was chosen for the present version of this model is based only on the variables update.

For a semi-implicit two-phase flow model the solution matrix is expressed in terms of pressure only. Other independent variables are updated in the back-substitution step. In that case it is usually sufficient to check the relative pressure update to satisfy the convergence. The convergence criterion is simply the following:

$$\max\left(\frac{\Delta P_i}{P_i}\right) \leq \varepsilon_n \tag{44}$$

The convergence tolerance varies from application to application. For example in COBRA-TF (Thurgood and George, 1983) ε_n is set to 10^{-3}.

For fully-implicit models the separation between the momentum equation and the mass and energy

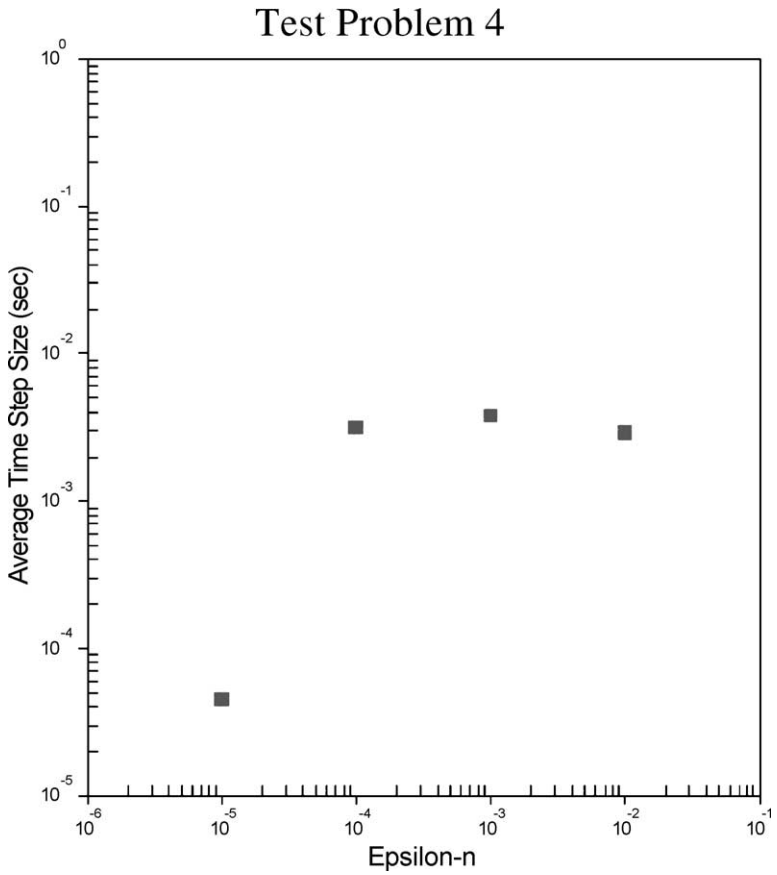

Fig. 5. Effect of the convergence tolerance coefficient (ε_n) on the average time step size.

equations is not possible. Phasic velocities are evaluated at different nodes and the solution matrix includes pressure, void fractions, enthalpies and velocities at the same time. Also in this case it is not necessary to check all variables' updates. For instance, mass and energy conservation is typically more important, while some errors in the solution of the momentum equations is tolerated. As a consequence in our model, the velocity update is neglected and the convergence criteria are limited to the updates of pressure, void fraction and enthalpies.

The use of the pressure as the only variable checked for the convergence was tested using Test Problem 4. The calculation diverged toward the end of the transient. This proved that, for a fully-implicit scheme, the convergence tests need to include updates of enthalpies and void fraction.

The selected criterion (Eq. (39)) is the result of numerical studies and it is a compromise between computational performance and accuracy. Numerical sensitivity studies were conducted based on Test Problem 4. Fig. 4 shows the effect of the convergence tolerance ε_n on conservation equation residuals. As expected the average residuals (errors) increase with the convergence tolerance. It was also found that a loose convergence criterion ($\varepsilon_n = 10^{-3}$ or 10^{-2}) causes the divergence to occur more frequently. The divergence forces more backups in the solution and a reduction in the average time step. Fig. 5 shows the effect of the convergence tolerance on the average

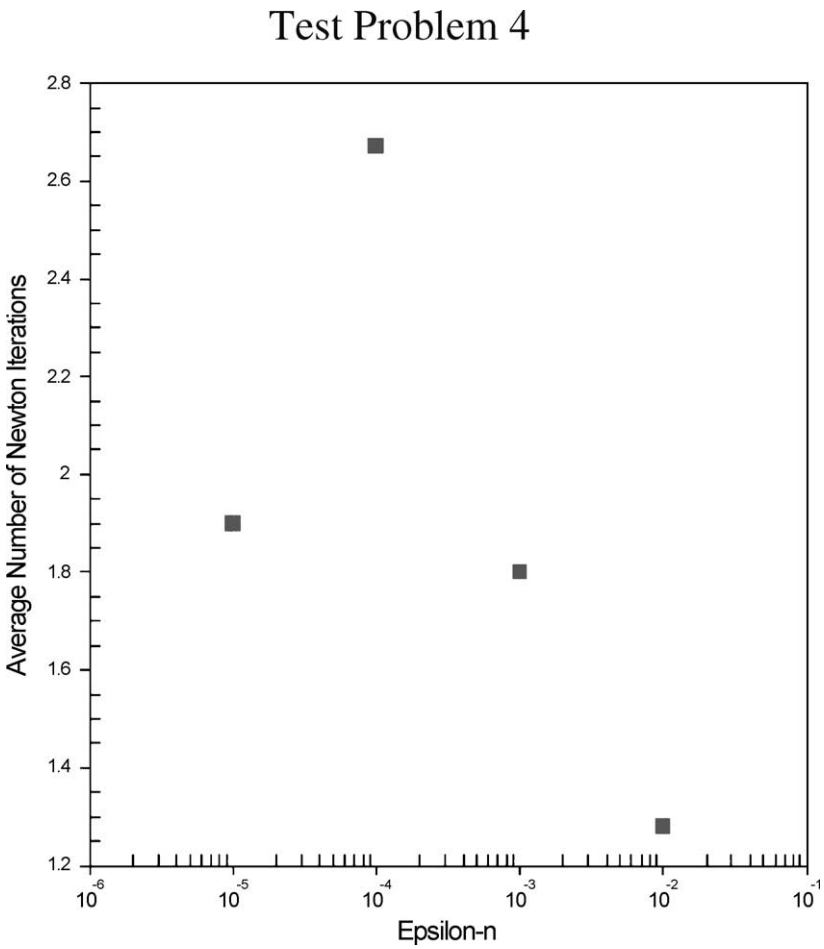

Fig. 6. Effect of the convergence tolerance coefficient (ε_n) on the average number of iterations per time step.

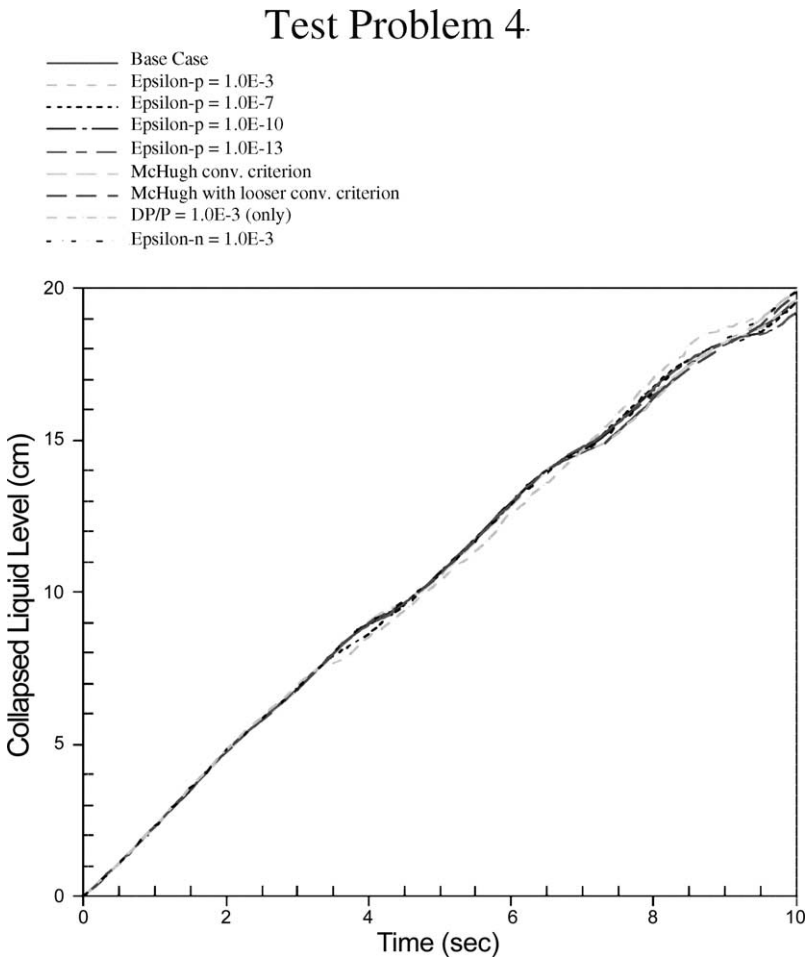

Fig. 7. Predicted collapsed liquid level for various sensitivity cases.

time step size. The effect on the average number of iterations required for a solution is shown in Fig. 6. The effect on the solution is small as shown in Fig. 7.

Therefore, from a pure computational performance standpoint, even if a reduced accuracy is acceptable, an excessively loose convergence criterion does not guarantee faster computations.

6.2. Time step size

An automatic time step size selection is implemented in the code. A Newton method converges quickly toward the solution as long as the initial guess is within the convergence radius. In a transient the solution at the previous time step is typically the best initial guess available. As we discussed in Section 4.1 predictor techniques help to better define the initial guess for some variables. Nevertheless it is in general true that the initial guess is closer to the final solution as the time step size is reduced. As a result the most obvious way to determine the optimum time step size is to examine the convergence history for the previous time steps. The user decides the maximum time step size depending on the time accuracy desired for a particular problem. Then during the transient an algorithm is used by the code to determine if the time step size can be increased toward the maximum value, needs to be reduced, or should stay the same in the current time step in order to keep the initial guess within the convergence radius.

Several techniques were explored and again the final selection (Eqs. (40) and (41)) was based on the performance of a number of calculations. The algorithm is based on the number of Newton iterations that were necessary to reach the convergence in the two previous time steps. If in both instances the number was less than or equal to three, the calculation is proceeding smoothly and the time step is increased by 10%. If the number of iterations in the previous time step was greater than seven or convergence was not reached at all, or worse the calculation diverged, the time step size is reduced by 50%. If the number of iterations in the previous time step is between 3 and 7 the time step, the calculation is at the limit of convergence and the time step size is not changed. Note that when the solution does not converge or diverges, the solution procedure is 'backed-up' (i.e. the calculation of the time step is repeated with a smaller time step).

It was observed that this time step logic combined with the convergence criteria allowed the calculation to advance in general with 2–3 Newton iterations per time step. A numerical study was conducted using Test Problem 4. The time step size reduction rate, for the case when convergence is not achieved, was reduced from 50 to 90%. The effect was that the average time step size used during the transient calculation increased by about 30%, however at the price of many more backups, and a less efficient computation.

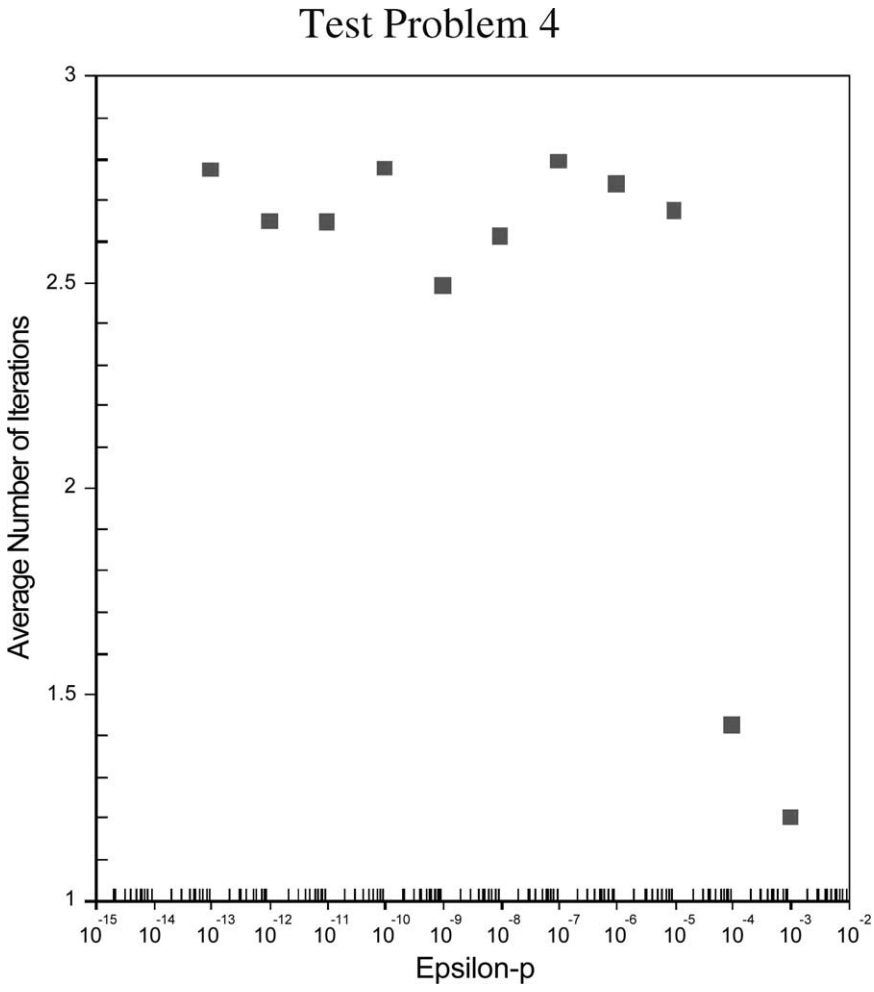

Fig. 8. Effect of ε_p on the average time step size.

6.3. Numerical evaluation of the Jacobian

As already discussed the evaluation of the Jacobian for a fully-implicit scheme becomes rather cumbersome. Here the Jacobian is evaluated numerically. This technique provides greater flexibility to the developer but has some shortcomings, which need further considerations. The partial derivatives are approximated by the following ratio:

$$\frac{\partial f_j}{\partial x_i} = \frac{f_j(x_1, x_2, \ldots, x_i + \delta x_i, \ldots, x_n) - f_j(x_1, x_2, \ldots, x_i, \ldots, x_n)}{\delta x_i} \quad (45)$$

where δx_i is a small perturbation to the independent variable x_i.

Using this method, instead of resolving the analytical derivatives and compiling the resulting expression into the code, the same routines are used with a different value for the set of independent variables. The perturbations δx_i should be small enough such that the local derivative is well-approximated by the previous ratio, but large enough to limit the effect of the round-off errors. In the Newton method, an error in the estimate of the Jacobian elements leads to slow convergence of the iteration.

Here the following expression is used to determine the magnitude to the perturbation to each independent

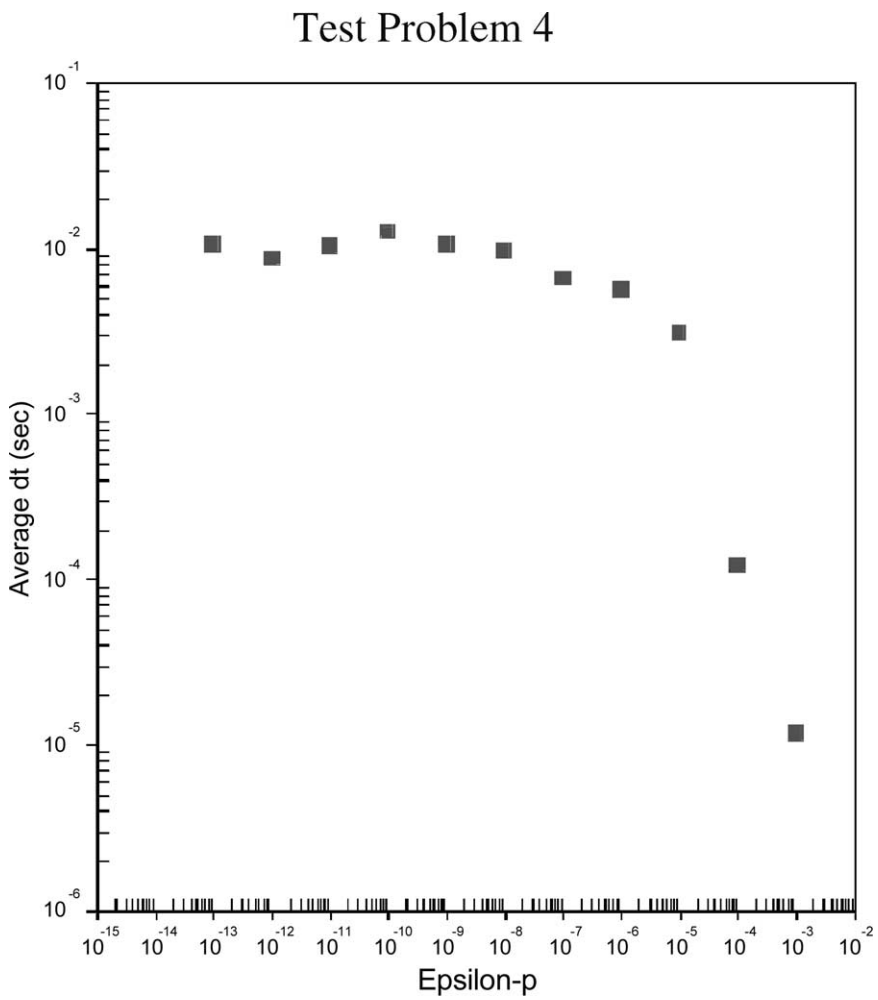

Fig. 9. Effect of ε_p on the average number of iterations per time step.

variable:

$$\begin{aligned}\delta P &= \varepsilon_p P\\ \delta\alpha &= 100\varepsilon_p\\ \delta H &= \varepsilon_p H\\ \delta v &= 100\varepsilon_p\,(\mathrm{m/s})\\ \delta T &= 100\varepsilon_p\,(\mathrm{K})\end{aligned} \tag{46}$$

Other authors (McHugh, 1995) suggested similar procedures. They suggested that the perturbation should be of the order of the square root of computer round-off errors. Here a numerical sensitivity study was conducted to investigate the effect of the multiplier ε_p.

Several runs have been performed with Test Problem 4 where the multiplier ε_p was varied from 10^{-3} to 10^{-14}. Fig. 7 shows the collapsed liquid level time history for several sensitivity cases. The collapsed liquid level, or the stored mass time history in a channel undergoing a reflood transient is often selected as an indicator of the global thermal-hydraulic transient response of the system. Fig. 7 shows that the global solution is not significantly affected by the value of the multiplier. On the other hand, it was found that the selection of ε_p does affect the robustness and stability of the calculation. The efficiency of the numerical method was inferred by examining the average time step size and the average number of iterations for each

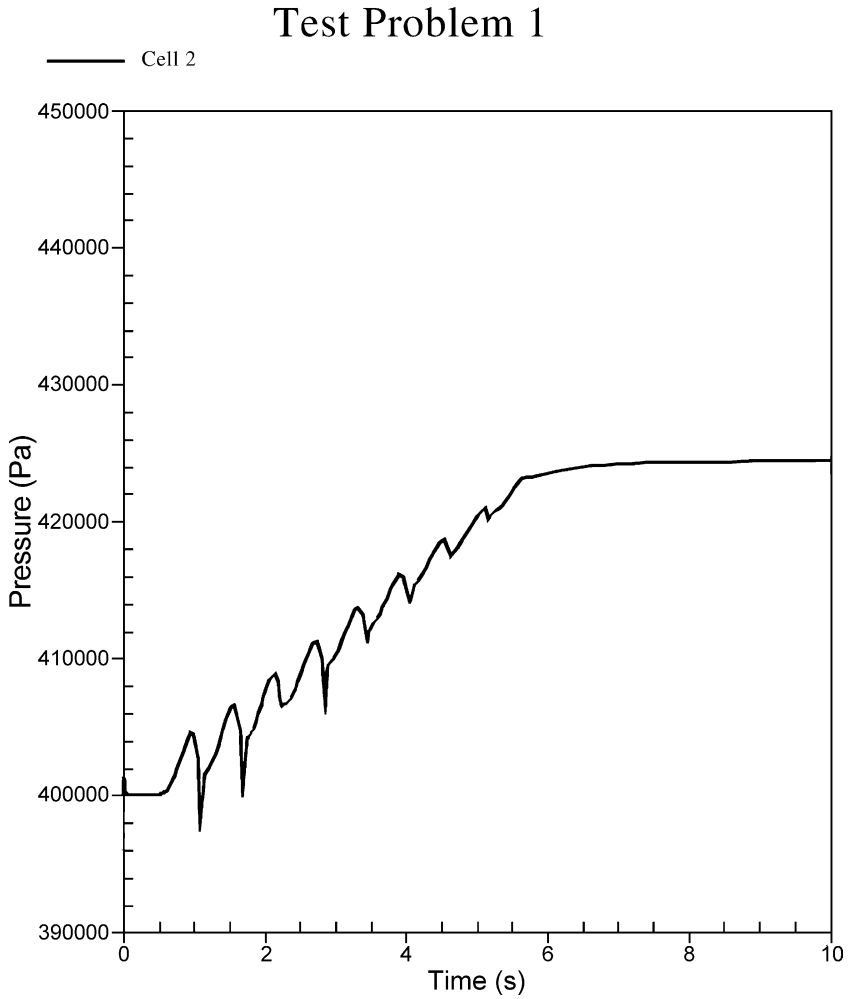

Fig. 10. Predicted pressure at the bottom of the channel.

time step. Based on the discussions in the previous sections about the time step size selection logic and convergence criteria, the increase in robustness can be seen as the increased average time step size and the decrease in the number of iterations per time steps.

Fig. 8 shows that the effect of the multiplier on the number of iterations per time step is small. The effect is more significant on the average time step size (Fig. 9). For this problem, the average time step increases for smaller values of ε_p and reach a maximum value when $\varepsilon_p = 10^{-10}$. Note that the time step is virtually insensitive to ε_p for $\varepsilon_p < 10^{-7}$. This is an indication that at smaller values, the effect of computer round-off errors becomes significant and tends to offset the possible accuracy for using ε_p in Eq. (45) for the evaluation of derivative. At the left extreme, when $\varepsilon_p = 10^{-14}$ the Jacobian matrix was calculated to be singular and solution was not reached. Dennis and Schnabel (1996) suggests a method to calculate the optimum value of ε_p based on the square root of round-off error. The round-off error can be calculated by examining how many significant digits there are in the mantissa. Note that the code was compiled in double-precision. On a 32 bit machine in double-precision, the mantissa contains typically 16 digits and the round-off error can be estimated to be of the order of 10^{-16}. Based on Dennis and Schnabel's (1996) suggestion a good value for ε_p would be the

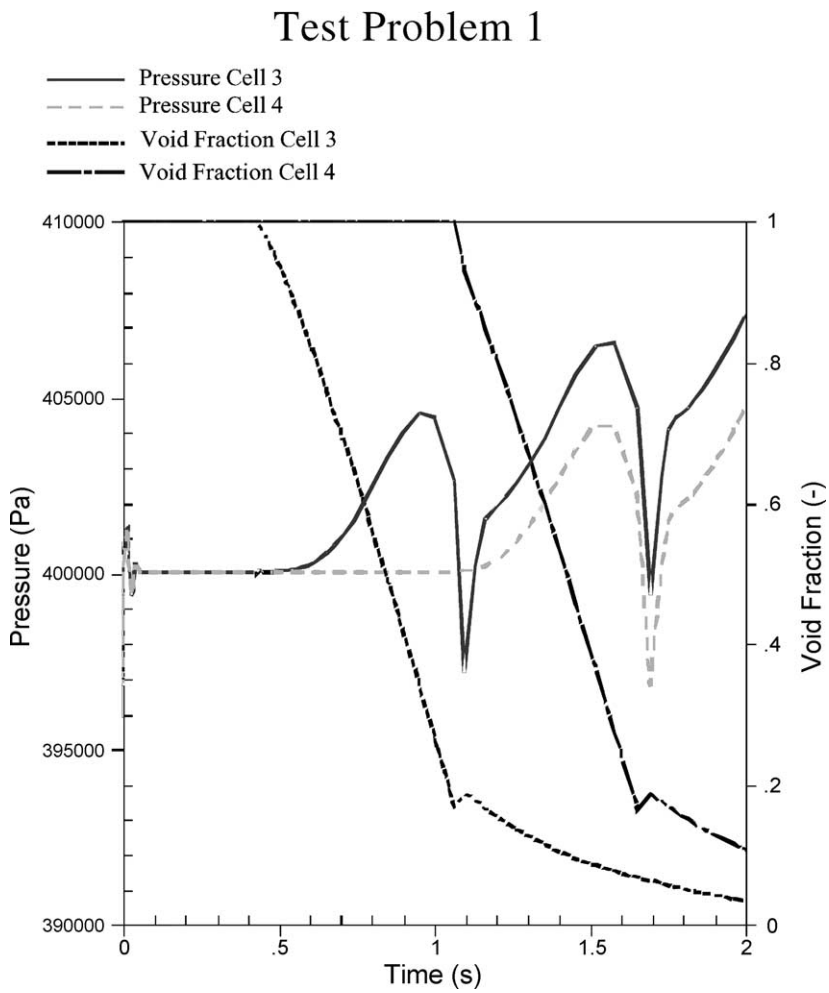

Fig. 11. Pressure and void fraction in the first two cells.

square root of the round-off error, which in this case gives $\varepsilon_p = 10^{-8}$. Therefore Dennis' method is in good agreement with the previous numerical results.

6.4. Initial guess and selection of equation set

For most of the variables the initial guess at the beginning of the time step is based on the solution of the previous time step. For the void fraction an 'improved' guess value is obtained solving Eqs. (36)–(38). Depending on the void fraction determined with the explicit predictor technique, different equation sets are used consistently with two-phase or single-phase flow. Some difficulties arise when the liquid velocity changes sign during a Newton iteration. In this event because of the donoring scheme the mass and energy equations' residuals are subjected to a sudden change. Also initial guess and selected equation set are not consistent with the final solution. Often calculations do not converge or diverge and time step size needs to be significantly reduced to bring back the initial guess within the convergence radius.

A partial fix to this problem was developed. The convergence criterion is relaxed in the event the liquid

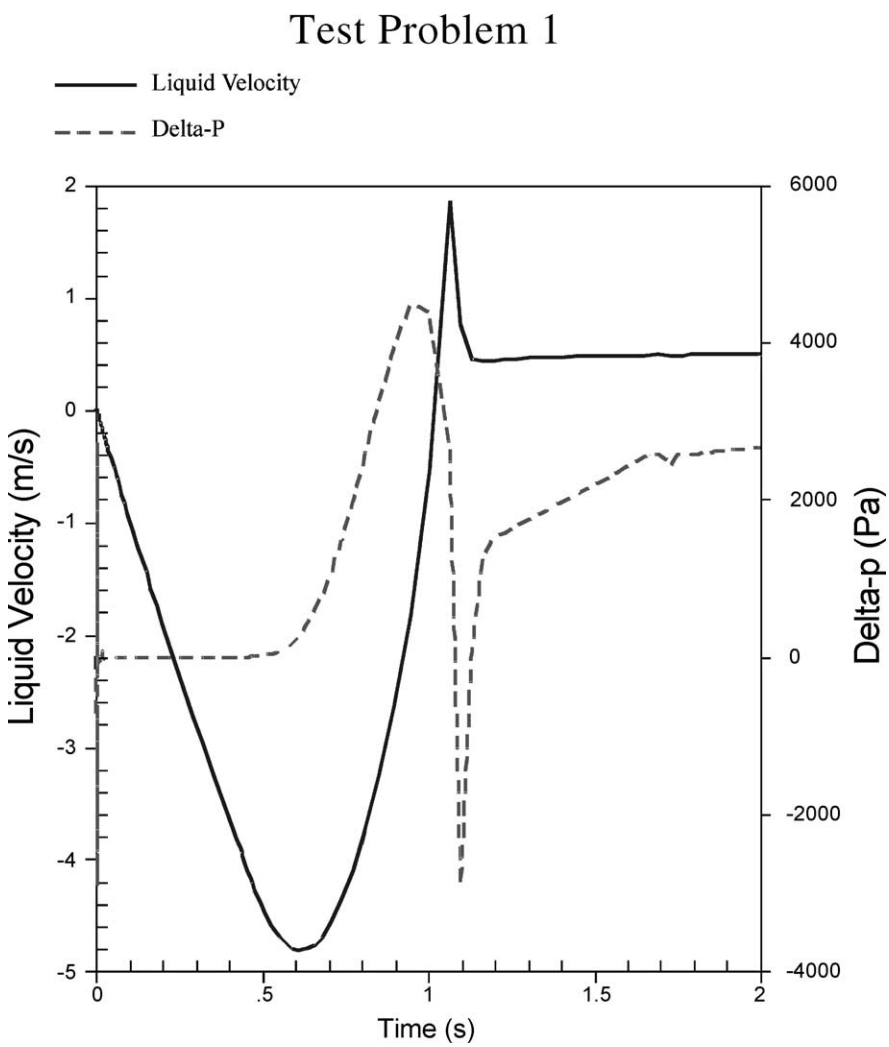

Fig. 12. Liquid velocity and differential pressure.

velocity changes sign. This allows the time step to be completed. The solution proceeds to the following time step while the convergence criterion is reset to its original value. Although this technique appears to work sometimes and has some benefits, it is not the final solution to this problem.

6.5. Determination of heat transfer regime

The heat conduction solution and the heat transfer from the wall to the fluid are implicitly coupled with the fluid flow solution (Section 3). The heat transfer coefficients are evaluated at the new time level as well as the wall temperature. One difficulty arises from the fact that the heat transfer coefficients can be determined only after selection of the boiling heat transfer regime, which is a function of the wall temperature and is also unknown. Moreover the heat transfer regime is determined only after knowing the CHF and minimum film boiling temperature (T_{min}) points in the boiling curve. In particular the CHF is a function of the unknown flow conditions and so is the wall temperature at the CHF point. Common instabilities occur because of treatment of the CHF point (Shieh et al., 1994).

Here, to simplify the problem, but retaining the implicit treatment as much as possible it was decided to use the old time value of the wall temperature for the determination of the heat transfer regime. Also the CHF is determined only during the first Newton iteration (at the beginning of the time step) and kept constant for all subsequent iterations. The evaluation of the CHF is basically explicit.

6.6. Explicit solution of interfacial area transport equation

Another simplification in the current version of the code is related to the treatment of the interfacial area transport equation (Eq. (10)). The equation could be added directly to the list of the fluid flow and wall to

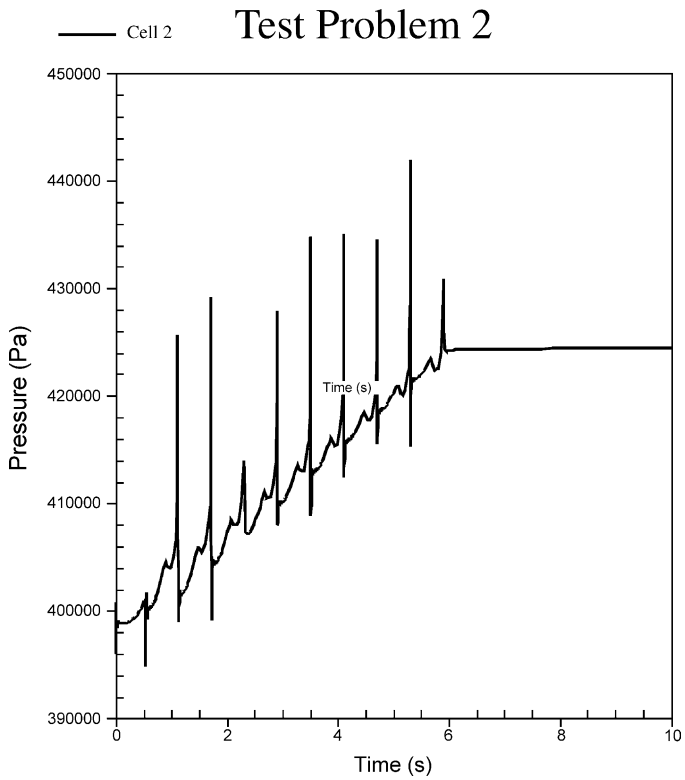

Fig. 13. Predicted pressure at the bottom of the channel.

fluid heat transfer equations. The expanded equation set can be solved including the interfacial area concentrations as additional unknowns. However, in the preliminary implementation of the code, it was decided for simplicity to have an explicit evaluation of the interfacial area for the dispersed droplet flow field. This is retained in the current version and the interfacial area concentration is solved with an explicit step after the fluid flow solution.

Eq. (10) is discretized with an explicit scheme. The time step used to solve the interfacial area transport equation is internally subdivided in fractional time steps. This was necessary because the material Courant limit applies to the explicit discrete equation derived from Eq. (10).

6.7. Unresolved issues

The model was tested against standard numerical problems (Test Problems 1–3). These are numerical benchmarks with solutions available analytically or can be compared to other numerical tests in the open literature.

The analytical solution to Test Problem 1 is straightforward. The liquid level rises at a constant rate and the pipe is full in 6.0 s. The pressure at the bottom of the pipe reaches a plateau, which corresponds to the gravity head of a 0.3 m column of saturated liquid at 400 kPa. Fig. 10 shows that on the average the predictions are correct. However, the numerical solution presents pressure oscillations corresponding to the time when the mixture level crosses the cell boundaries. Fig. 11 shows in detail the first 2 s of transient, including the pressure in the second and third cells together with the void fraction. Pressure in a cell starts to increase as soon as the liquid appears in the cell. The rate of increase in pressure is higher than the gravity head component. Fig. 12 shows the liquid velocity at the junction between cells 3 and 4 together with the pressure difference between the two nodes. The figure

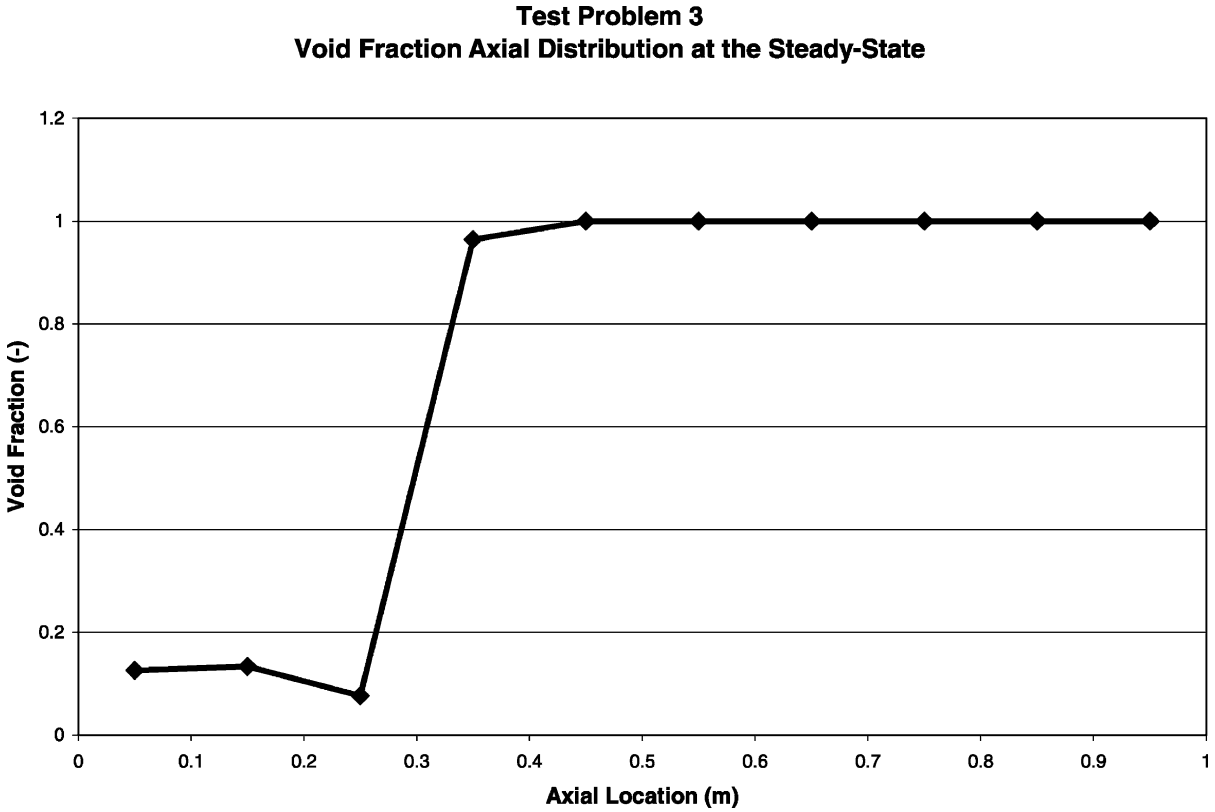

Fig. 14. Void fraction axial profile.

clearly shows that the pressure rise is higher than the gravity head gained. This is the effect of the momentum of the fluid that is accelerated starting at about 0.5 s. The liquid velocity reaches a maximum (see positive spike in Fig. 12) and then relaxes toward a constant value, which corresponds to the single-phase liquid velocity solution. The differential pressure has a negative spike before returning to the value which corresponds to the gravity head component. This phenomenon is known (Aktas and Mahaffy, 1996) and the observed transient behavior is due to the inability of the numerical model to capture the physical position of the mixture level.

Test Problem 2 combines the previous phenomenon with the effect of the vapor condensation at the top of the liquid level. Fig. 13 shows the pressure in the first cell of the channel. A large positive pressure spike is seen at the time the level crosses the cell boundary and propagates through the system. The pressure spike is due to a 'water packing' phenomenon. Stewart and Wendroff (1984) suggested that the 'water packing' problem is typical of semi-implicit models. However the present fully-implicit model shows that this is a more common numerical issue than they indicated. This is consistent with the results from Mahaffy and Liles (1983). In their work on water packing they clearly indicated that this pressure spike behavior is inevitable in any Eulerian codes. The magnitude of the pressure spikes appears to be less severe with a fully-implicit scheme because the time step size used

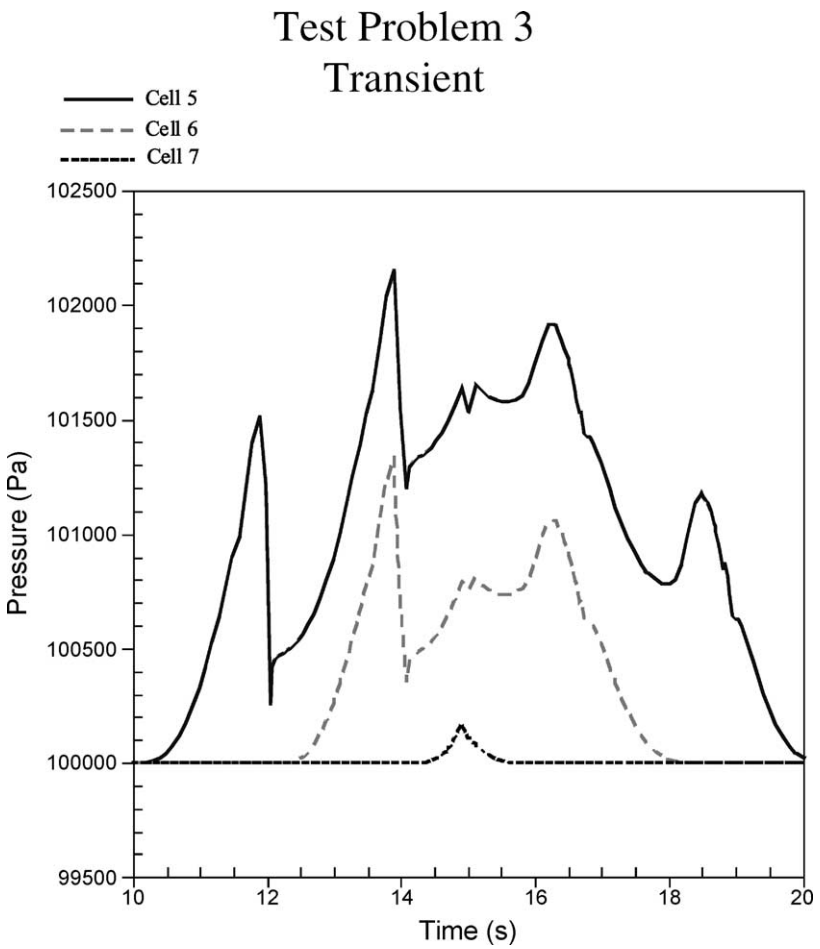

Fig. 15. Predicted pressure.

in the calculation is larger. As indicated by Mahaffy and Liles (1983), water packing is peculiar in that the answer gets worse as the time step gets smaller. One solution to the problem can be found in Pryor et al. (1978) and Mahaffy and Liles (1983). They showed that pressure spikes can be suppressed with a temporary artificial reduction of the inertia of the fluid when a cell nears a filling point. This allows the velocity to quickly adjust to the proper value.

Test Problem 3 is a repetition of the numerical exercise used by Aktas and Mahaffy (1996) to test the implementation of a two-phase level tracking method in the TRAC-BWR code. In this test the first 10 s are used to establish a steady-state condition by injecting steam at the bottom of a layer of water. Fig. 14 shows the void fraction profile calculated at the end of the steady-state period. At 10 s a constant liquid flow rate is injected for 5 s and then is withdrawn for other 5 s. Fig. 15 shows the pressure transient for cells 5–7 predicted by this fully-implicit model. Fig. 16 shows the predicted void fraction for the same cells while Fig. 17 shows the phasic velocities at the junction between the two control volumes. The pressure is subjected to oscillations as the mixture level crosses the cell boundaries. The calculated oscillations are similar in nature to the ones described for Test Problem 1 and the oscillations discussed in the work of Aktas and Mahaffy (1996). The pressure increases at a high rate because liquid is accelerated at the cell boundary. The magnitude of the oscillations is less than the one

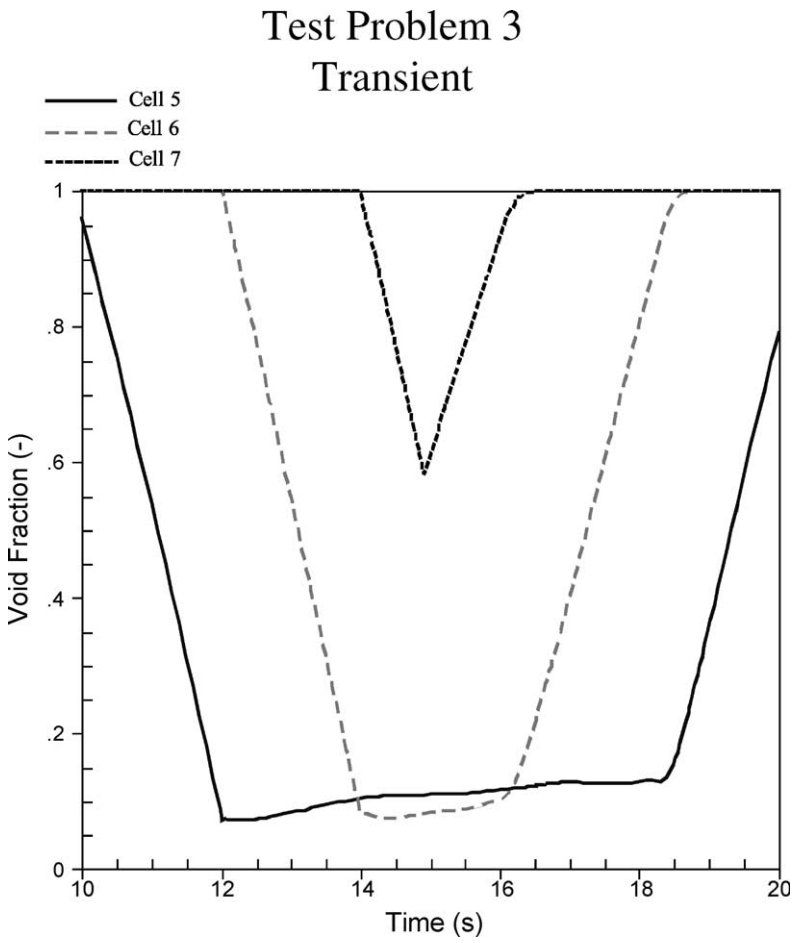

Fig. 16. Predicted void fraction.

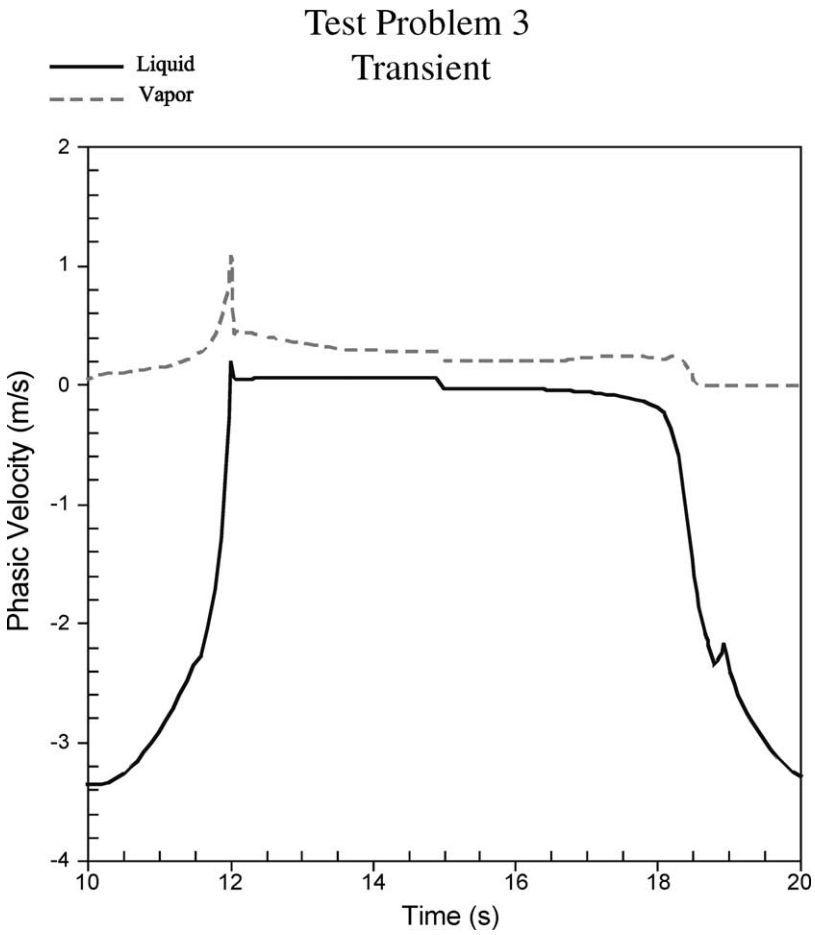

Fig. 17. Vapor and liquid velocity.

observed with the original version of TRAC used by Aktas and Mahaffy (1996). Our results indicate that a similar mixture liquid level tracking method should be able to eliminate this problem.

7. Closing remarks on robustness and computational performance

The robustness of the model was tested successfully varying various parameters within the range of interest. Also the effect of modeling parameters such as the convergence tolerance, the converge criteria, the magnitude of the perturbation used to evaluate numerically the Jacobian have been studied using Test Problem 4. Fig. 7 shows that the effect on the solution is limited.

The numerical evaluation of the Jacobian has many advantages but it can be computationally expensive. On the average between 2 and 3 Newton iterations are necessary to solve each time step. For the same mesh size, the average time step size is larger than the time step size that can be used with a semi-implicit model but only to some extent. As a result, for the applications of interest, the fully-implicit model is probably computationally more expensive than an equivalent semi-implicit model. On the other hand the model is quite more robust and a stable and non-oscillatory solution can be achieved with a grid resolution that is prohibitive for a semi-implicit method.

The flexibility provided by the numerical evaluation of the Jacobian is attractive for further developments of this program. One is the investigation of higher order

numerical schemes, which increases the complexity and extent of non-zero off-diagonal elements in the Jacobian. However, in a production code a balance of convenience and speed must be achieved. Evaluation of the Jacobian by a mixture of analytic and numerical methods is probably the most efficient approach.

As a final note, time-smoothing procedures applied to interphase exchange terms or similar numerical techniques are necessary in a semi-implicit model to achieve a stable solution. These are eliminated from the current fully-implicit method. This is an important advantage over the semi-implicit schemes. Often these techniques are regarded more as an 'art' than science, means to make the code work. They put the analyst in the difficult position to justify the use of such numerical strategies necessary to complete calculations. The effect of these ad hoc procedures on the solution is not clear and often needs to be assessed with extensive sensitivity studies.

8. Conclusions

The development and implementation of a fully-implicit model to describe the complex two-phase flow behavior in the quench front region of a reactor core has been described.

The development of various techniques for the solution of the equation set, such as the converge criteria, the time step logic, the initial guess, etc. has been discussed in detail and provides insights for further development of this model or other similar models.

The numerical evaluation of the Jacobian proved to be a valuable technique, which significantly simplified the implementation of a fully-implicit method, especially with many equations involved. The development of an algorithm able to handle the transition to the single-phase regime was another breakthrough during the development of this model.

The model proved to be robust, and as a result a relatively large time step could be used during the solution of the quench front flow problem using a very fine hydraulic mesh. There are some unresolved numerical issues in the current version of the code, which need to be considered for further development. Results indicated that a resolution to the water packing phenomenon and a water level tracking model might be needed to improve further the results. These problems are typical for most of the current thermal-hydraulic codes and solution options are known.

Acknowledgements

The work presented in this paper was made possible thanks to the financial support from the U.S. Nuclear Regulatory Commission.

References

Aktas, B., Mahaffy, J.H., 1996. A two-phase level tracking method. Nucl. Eng. Des. 162, 271–280.

Arai, M., 1980. Characteristic and stability analyses for two-phase flow equation systems with viscous terms. Nucl. Sci. Eng. 74, 77–83.

Banerjee, S., Chan, A.M.C., 1980. Separated flow models—I. Analysis of the averaged and local instantaneous formulations. Int. J. Multiphase Flow 6, 1–24.

Bestion, D., 1990. The physical closure laws in CATHARE code. Nucl. Eng. Des. 124, 229.

Dennis, J.E., Schnabel, R.B., 1996. Numerical Methods for Unconstrained Optimization and Nonlinear Equations. SIAM.

Frepoli, C., 2001, Development of a Subgrid Model with a Fine Moving Grid Overlying a Coarse Eulerian Mesh for Modeling Reflood Heat Transfer. PhD Thesis.

Frepoli, C., Hochreiter, L.E., Mahaffy, J., Cheung, F.B., 2000. A noding sensitivity analysis using COBRA-TF and the effect of spacer grids during core reflood. In: Proceedings of ICONE 8, 8th International Conference on Nuclear Engineering, Baltimore, USA.

Gidaspow, D., 1974. Introduction to "modeling of two-phase flow." In: Round Table Discussion (RT-1-2), Proceedings of the Fifth International Heat Transfer Conference, vol. VII, p. 163.

Golub, G., Ortega, J.M., 1993. Scientific Computing, An Introduction With Parallel Computing. Academic Press, Inc.

Hewitt, G.F., Delhaye, J.M., Zuber, M., 1992. Multiphase Science and Technology, vol. 6.

Hibiki, T., Ishii, M., 2001. Development of one-group interfacial area transport equation in bubbly flow systems. Int. J. Heat Mass Transfer 45, 2351–2372.

Ishii, M., Mishima, K., 1982. Two-fluid model and hydrodynamic constitutive relations. Nucl. Eng. Des. 82, 107–126.

Katsma, K.R., Paulsen, Hughes, E.D., 1985. An implicit numerical solution method for the RETRAN thermal-hydraulic transient code. In: Proceedings of the Twenty-thirrd ASME/AICHE/ANS National Heat Transfer Conference.

Kelly, J.M., Stewart, C.W., Cuta, J.M., 1992. VIPRE-02—a two-fluid thermal-hydraulic code for reactor core and vessel analysis: mathematical modeling and solution methods. Nucl. Technol. 100.

Krishnamurthy, R., Ransom, V.H., 1992. A non-linear stability study of the RELAP5/MOD3 two-phase model. In: Proceedings

of the Japan-US Seminar on Two-Phase Flow Dynamics, Berkeley, California.

Lahey, R.T., Drew, D.A., 1990. The current state-of-the-art in the modelling of vapor/liquid two-phase flows. In: Proceedings of the ASME Winter Annual Meeting, November 25–30.

Lahey, R.T., Cheng, L.Y., Drew, D.A., Flaherty, J.E., 1980. The effect of virtual mass on the numerical stability of accelerating two-phase flow. Int. J. Multiphase Flow 6, 281–294.

Lee, N., Wong, S., Yeh, H.C., Hochreiter, L.E., 1981. PWR FLECHT-SEASET Unblocked Bundle Forced and Gravity Reflood Task Data Evaluation and Analysis Report. NUREG/CR-2256.

Liles, D.R., Reed, W.H., 1978. A semi-implicit method for two-phase fluid dynamic. J. Comput. Phys. 26, 390–407.

Loftus, M.J., et al., 1980. PWR FLECHT-SEASET Unblocked Bundle Forced and Gravity Reflood Task Data Report. NUREG/CR-1532.

Lyczkowski, R.W., 1980. An analysis of why single pressure two-fluid two-phase unequal velocity model equations are not globally hyperbolic. Nucl. Sci. Eng. 76, 246–257.

Lyczkowski, R.W., Gidaspow, D., Solbrig, C.W., Hughes, E.D., 1978. Characteristics and stability analyses of transient one-dimensional two-phase flow equations and their finite difference approximations. Nucl. Sci. Eng. 66, 378–396.

Mahaffy, J.H., 1982. A stability-enhancing two-step method for fluid flow calculations. J. Comp. Phys. 46, 329–341.

Mahaffy, J.H., Liles, D.R., 1983. Numerically induced pressure excursions in two-phase-flow calculations. In: Proceedings of the Second Annual Topical Meeting on Nuclear Thermal Hydraulics, Santa Barbara, California.

McHugh, P.R., 1995. An investigation of Newton-Krylov Algorithms for Solving Incompressible and Low Mach Number Compressible Fluid Flow and Heat Transfer Problems Using Finite Volume Discretization. INEL-95/0118.

No, H.C., Kazimi, M.S., 1985. Effects of virtual mass on the mathematical characteristics and numerical stability of the two-fluid model. Nucl. Sci. Eng. 89, 197–206.

Paik, C.Y., Hochreiter, L.E., Kelly, J.M., Kohrt, R.J., 1985. Analysis of FLECHT-SEASET 163-Rod Blocked Bundle Data using COBRA-TF. NUREG/CR-4166.

Pokharna, H., Mori, M., Ransom, V.H., 1997. Regularization of two-phase flow models: a comparison of numerical and differential approaches. J. Comput. Phys. 134, 282–295.

Pryor, R.J., Liles, D.R., Mahaffy, J.H., 1978. Treatment of water packing effects. Trans. ANS 30, 208–209.

Rajamaki, M., 1996. Elimination of numerical diffusion in 1-phase and 2-phase flows. In: Trans. OECD/NEA/CSNI Workshop on Transient Thermal-Hydraulic and Neutronic Code Requirements, Annapolis, USA.

Ramshaw, J.D., Trapp, J.A., 1978. Characteristics, stability, and short-wavelength phenomena in two-phase flow equation systems. Nucl. Sci. Eng. 66, 93.

Ransom, V.H., Hicks, D.L., 1984. Hyperbolic two-pressure models for two-phase flow. J. Comput. Phys. 53, 124.

RELAP5 Code Development Team, 1995a. RELAP5/MOD3 Code Manual: Code Structure, System Models, and Solution Methods. NUREG/CR-5535.

RELAP5 Code Development Team, 1995b. RELAP5/MOD3 Code Manual Volume V: Models and Correlation. NUREG/CR-5535.

Shieh, A.S.L., Krishnamurthy, R., Ransom, V.H., 1994. Stability, accuracy, and convergence of the numerical methods in REALAP5/MOD3. Nucl. Sci. Eng. 116, 227–244.

Schnurr, N., et al., 1990. "TRAC-PF1/MOD2 User's Guide," Nuclear Technology and Engineering Division, Engineering Safety Analysis Group N-6, Los Alamos National Laboratory.

Song, J.H., Ishii, M., 2001a. On the stability of one-dimensional two-fluid model. Nucl. Eng. Des. 204, 101–115.

Song, J.H., Ishii, M., 2001b. The one-dimensional two-fluid model with momentum flux parameters. Nucl. Eng. Des. 205, 145–158.

Stewart, H.B., Wendroff, B., 1984. Review article: two-phase flow: models and methods. J. Comput. Phys. 56, 363–409.

Stuhmiller, J.H., 1977. The influence of interfacial pressure forces on the character of two-phase flow model equations. Int. J. Multiphase Flow 3, 351–560.

Tannehill, J.C., Anderson, D.A., Pletcher, R.H., 1997. Computational Fluid Mechanics and Heat Transfer. Taylor&Francis.

Thurgood, M.J., George, T.L., 1983. COBRA/TRAC—A Thermal-Hydraulic Code for Transient Analysis of Nuclear Reactor Vessels and Primary Coolant System. NUREG/CR-3046, vols. 1–4.